Wind and Structures, Vol. 8, No. 6 (2005) 407-426
DOI: http://dx.doi.org/10.12989/was.2005.8.6.407

Hybrid RANS/LES simulations of a bluff-body flow

S. Camarri† and M.V. Salvetti‡

Dipartimento di Ingegneria Aerospaziale, Università di Pisa, Italy

B. Koobus‡†

Département de mathématiques, Université de Montpellier II, France

A. Dervieux‡‡

INRIA Sophia-Antipolis, France

(Received February 7, 2005, Accepted October 10, 2005)

Abstract. A hybrid RANS/LES approach, based on the *Limited Numerical Scales* concept, is applied to the numerical simulation of the flow around a square cylinder. The key feature of this approach is a blending between two eddy-viscosities, one given by the $k-\varepsilon$ RANS model and the other by the Smagorinsky LES closure. A mixed finite-element/finite-volume formulation is used for the numerical discretization on unstructured grids. The results obtained with the hybrid approach are compared with those given by RANS and LES simulations for three different grid resolutions; comparisons with experimental data and numerical results in the literature are also provided. It is shown that, if the grid resolution is adequate for LES, the hybrid model recovers the LES accuracy. For coarser grid resolutions, the blending criterion appears to be effective to improve the accuracy of the results with respect to both LES and RANS simulations.

Keywords: hybrid RANS/LES modeling; limited numerical scales; square-cylinder flow.

1. Introduction

The most widely used approach for the simulation of high-Reynolds number turbulent flows is the one based on the Reynolds-Averaged Navier-Stokes equations (RANS). In the RANS approach, an averaging procedure is applied to the Navier-Stokes equations; thus, only the averaged flow is directly simulated, while a closure model provides the effects of turbulent fluctuations. This leads to a noticeable simplification of the problem and, consequently, to moderate simulation costs, which are almost independent of the Reynolds number, when it is sufficiently large. However, RANS models usually have difficulties in accurately predicting the flow around bluff-bodies. Indeed,

† Professor, Corresponding Author, E-mail: mv.salvetti@ing.unipi.it
‡ Post-doc, E-mail: s.camarri@ing.unipi.it
‡† Assistant Professor, E-mail: koobus@math.univ-montp2.fr
‡‡ Research Director, E-mail: Alain.Dervieux@sophia.inria.fr

although successful RANS simulations of bluff-body flows on very fine grids are reported in the literature (see, for instance, Kato and Launder 1993, Durbin 1995), usually RANS models give an excessive dissipation and do not properly take into account 3D phenomena, yielding significant discrepancies with the experimental results.

An alternative to the RANS approach is the large-eddy simulation (LES), which consists in directly simulating the scales larger than a given dimension and in modeling the effect of the unresolved scales on the remaining ones (SGS modeling). Since the dynamics of the large turbulent scales is directly simulated and three-dimensionality and unsteadiness are naturally taken into account, LES results are generally more accurate than those of RANS simulations for bluff-body flows. However, LES simulations are characterized by computational costs much larger than in the RANS case. Moreover, the computational requirements significantly increase with the Reynolds number, because, to obtain reliable results in LES simulations, the grid has to be fine enough to resolve a significant part of the turbulent scales. This becomes particularly critical in the near-wall region (see, for instance, Bagget, *et al*. 1997).

A relatively recent class of new turbulence models, known as hybrid RANS/LES models, has been proposed. This name indicates approaches which may be very different but which share the idea of combining the LES and the RANS methodologies within the same simulation, in order to obtain the same accuracy as in LES at reasonable computational costs.

One of the possible strategies to couple RANS and LES is the *blending strategy*, leading to the so called *universal models*, in which the two approaches are blended together in a continuous way throughout the domain.

Among the *universal models* described in the literature, the Detached Eddy Simulation (DES) has received the largest attention. This approach, proposed by Spalart, *et al*. (1997), is based on the Spalart-Allmaras RANS model (1994), in which the length scale of the turbulent kinetic energy destruction term is modified to be the minimum between the distance to the wall and a length proportional to the largest of the local grid spacing in the three-directions. Thus, in the near-wall region and with RANS-like grids the Spalart-Allmaras RANS model is used, while far from the wall the simulation switches in the LES mode with a one-equation SGS closure.

The DES approach has successfully been used in several applications described in the literature (see, for instance, Breuer, *et al*. 2003, Constantinescu, *et al*. 2002, Constantinescu and Squires 2003, Hedges, *et al*. 2002, Kotapati-Apparao and Squires 2003, Shur, *et al*. 1999, Travin, *et al*. 2000 for bluff-body flows), and, thus, it is probably at present the most validated hybrid RANS/LES approach.

Another class of methods is based on the idea, introduced by Speziale (1998), of multiplying the Reynolds stress tensor coming from a RANS model by a *blending* parameter, which depends on the local grid resolution; in particular, it is lower than one where the grid is sufficiently refined, leading to a damping of the RANS model. The model proposed by Speziale has been scarcely used, probably because the blending parameter implies the computation of the Kolmogorov length-scale, which is not trivial for most flows.

In the Limited Numerical Scales (LNS) approach, recently proposed by Batten (Batten, *et al*. 2004, Batten 2002, Batten, *et al*. 2001), the blending parameter depends on the values of the eddy-viscosity given by a RANS model, μ_t, and of the SGS viscosity given by a LES closure, μ_s. In practice, the minimum of the two eddy-viscosities is used. This should ensure that, where the grid is fine enough to resolve a significant part of the turbulence scales, the model works in the LES mode, while elsewhere the RANS closure is recovered. For a deeper discussion of the motivations leading to the LNS approach and of the physical meaning of the blending criterion we refer to Batten, *et al.* (2004).

The starting point of the present work is a numerical solver (AERO) for the Navier-Stokes equations in the case of compressible flows and perfect Newtonian gases, based on a mixed finite-element/finite-volume scheme formulated for unstructured grids made of tetrahedral elements. Finite elements (P1 type) and finite volumes are used to treat the diffusive and convective fluxes, respectively. The code AERO has been extensively used for RANS simulations of many different flows (see, for instance, Farhat, *et al.* 1999, Koobus, *et al.* 2000), with the standard $k-\varepsilon$ closure model (Launder and Spalding 1979). More recently a LES approach has also been implemented in AERO, with different closure models (Camarri, *et al.* 2002b, Koobus and Farhat 2004, Omari, *et al.* 2003), and has been applied to the simulation of different types of flows (see Camarri, *et al.* 2002b, Camarri, *et al.* 2004, Koobus and Farhat 2004 for bluff body flows).

In order to carry out hybrid RANS/LES simulations with AERO, the LNS approach is adopted. The motivations for this choice are twofold. First, the LNS approach does not require a specific RANS model. Indeed, although the basic RANS model of the LNS approach proposed by Batten, *et al.* (2004) is a non-linear $k-\varepsilon$ model, any eddy-viscosity RANS model might be used instead (see also Batten, *et al.* 2004), and this allowed us to exploit the already available and validated $k-\varepsilon$ closure. This also leaves the possibility of increasing the accuracy of the hybrid simulations by improving either the RANS or the LES closures. Second, the blending criterion in LNS depends only on the eddy and SGS viscosities, which are easy and inexpensive to be computed also on unstructured grids. Conversely, the evaluation of the distance from the wall, which is required in DES, is not trivial on unstructured grids and for complex geometries.

However, the LNS approach is still scarcely validated; to our knowledge it has been used only in Batten, *et al.* (2004), Batten (2002), Batten, *et al.* (2001). Thus, the present work gives a contribution to investigate whether the LNS blending criterion is effective for bluff-body flows, and for numerics and RANS and LES closures that are different from these adopted in Batten, *et al.* (2004), Batten (2002), Batten, *et al.* (2001). As for the latter point, since the LNS approach used in the present work is based on the standard $k-\varepsilon$ model (Launder and Spalding 1979), and becomes very similar to the Smagorinsky model for compressible flows in the LES mode (see Lenormand, *et al.* 2000), it is different from the one used by Batten, *et al.* (2004), who employed a non-linear $k-\varepsilon$ model instead of the standard one. The non-linear $k-\varepsilon$, which differs from the standard one mainly for the constitutive equation relating the time averaged flow to the Reynolds stress tensor by means of the turbulent eddy viscosity, has been shown to be definitely superior to the standard one for massively separated flows (see, for instance, Lakehal and Thiele 2001, Lubke, *et al.* 2001). Nonetheless, no ad-hoc re-calibration of the model constants (Abalakin, *et al.* 2003) nor local treatments, as the Menter correction (1993), have been adopted here for improving the standard $k-\varepsilon$, because the crucial point of this first investigation is, in our opinion, to assess whether the LNS concept is able to improve the prediction accuracy with respect to a given RANS model. The standard $k-\varepsilon$ model has been chosen as an example of standard RANS modeling available in most numerical codes used for engineering applications. We are aware that the global accuracy might be improved by using the LNS approach together with a RANS model that is more effective than the standard $k-\varepsilon$ one, but this point will be the object of further investigation.

To investigate the capabilities of the adopted hybrid approach, the flow around a square cylinder is considered, at Reynolds number, based on the far-field velocity and on the side length of the cylinder, equal to $Re=22000$. For this value of the Reynolds number, several experimental and numerical results, both from RANS and LES simulations, are available in the literature. Three sets of simulations carried out with three different grid resolutions are presented.

In the first one, a fine grid is used, which was already employed for LES simulations (see Camarri, *et al*. 2002b, Camarri, *et al*. 2004). This first set of simulations is aimed to verify whether on a sufficiently refined grid the LNS approach actually tends to LES.

The second and third sets of simulations are aimed to investigate the capabilities of the LNS approach in cases in which it is expected to work in both the RANS and LES modes; to this aim, the used grid resolution is progressively coarsened.

In all cases, the LNS results are compared with those obtained with the $k-\varepsilon$ RANS model, and with the LES Smagorinsky closure. Comparisons with experimental data and numerical results in the literature are also provided.

2. LNS approach

The Reynolds-Averaged Navier-Stokes equations for compressible flows of (calorically and thermally) perfect Newtonian gases are considered here, written in conservative form in the following variables: density (ρ), momentum (ρu_i, $i=1,2,3$) and total energy per unit volume ($E=\rho e+1/2\rho u_i u_i$, e being the internal energy).

The standard $k-\varepsilon$ model (Launder and Spalding 1979) is used for the closure of the RANS equations, in which the Reynolds stress tensor is modeled as follows, by introducing a turbulent eddy-viscosity, μ_t:

$$R_{ij} \simeq \mu_t \underbrace{\left[\frac{\partial \tilde{u}_i}{\partial x_j} + \frac{\partial \tilde{u}_j}{\partial x_i} - \frac{2}{3}\frac{\partial \tilde{u}_l}{\partial x_l}\delta_{ij}\right]}_{\tilde{P}_{ij}} - \frac{2}{3}\bar{\rho}k\delta_{ij}, \tag{1}$$

in which the tilde denotes the Favre average, the overbar time averaging, δ_{ij} is the Krönecker symbol and k is the turbulent kinetic energy. The turbulent eddy-viscosity μ_t is defined as a function of k and of the turbulent dissipation rate of energy, ε, as follows:

$$\mu_t = C_\mu \frac{k^2}{\varepsilon} \tag{2}$$

where C_μ is a model parameter, set here equal to the classical value of 0.09 and k and ε are obtained from the corresponding modeled transport equations (see Launder and Spalding 1979).

As already stated in the Introduction, in the LNS model the Reynolds stress tensor given by the RANS closure is multiplied by a blending function. Thus, the LNS equations are obtained from the RANS ones by replacing the Reynolds stress tensor R_{ij}, given by Eq. (1), with the tensor L_{ij}:

$$L_{ij} = \alpha R_{ij} = \alpha\mu_t\tilde{P}_{ij} - \frac{2}{3}\bar{\rho}(\alpha k)\delta_{ij}, \tag{3}$$

where α is the damping function ($0 \le \alpha \le 1$), varying in space and time.

In the LNS model proposed in Batten, *et al*. (2004), the damping function is defined as follows:

$$\alpha = \min\left\{\frac{\mu_s}{\mu_t}, 1\right\} \tag{4}$$

in which μ_s is the SGS viscosity obtained from a LES closure model. The Smagorinsky SGS model (1963) is adopted here; thus, we have:

$$\mu_s = \bar{\rho} C_s \Delta^2 \sqrt{\tilde{S}_{ij} \tilde{S}_{ij}} \tag{5}$$

where C_s is the model input parameter, $\tilde{S}_{ij}$ is the strain-rate tensor and Δ is a length which should be representative of the size of the resolved turbulent scales. Here, Δ has been selected, for each tetrahedral element of the grid, as the length of the longest edge (see Camarri, *et al.* 2002b) and C_s has been set equal to 0.01.

The set of LNS equations is reported here for sake of completeness:

$$\frac{\partial \bar{\rho}}{\partial t} + \frac{\partial \bar{\rho} \tilde{u}_i}{\partial x_i} = 0, \tag{6}$$

$$\frac{\partial \bar{\rho} \tilde{u}_i}{\partial t} + \frac{\partial \bar{\rho} \tilde{u}_i \tilde{u}_j}{\partial x_j} = -\frac{\partial \bar{p}}{\partial x_i} + \frac{\partial (\tilde{\sigma}_{ij} + L_{ij})}{\partial x_j}, \tag{7}$$

$$\frac{\partial \bar{E}}{\partial t} + \frac{\partial \tilde{u}_j (\bar{E} + \bar{p})}{\partial x_j} = \frac{\partial \tilde{u}_i \tilde{\sigma}_{ij}}{\partial x_j} + \frac{\partial \tilde{u}_i L_{ij}}{\partial x_j} + \frac{\partial}{\partial x_j}\left(\frac{\alpha \mu_t}{\sigma_k} \frac{\partial k}{\partial x_j}\right) + \frac{\partial}{\partial x_j}\left(\frac{C_p}{Pr}(\mu + \alpha \mu_t) \frac{\partial \tilde{T}}{\partial x_j}\right) \tag{8}$$

$$\frac{\partial \bar{\rho} k}{\partial t} + \frac{\partial \bar{\rho} \tilde{u}_j k}{\partial x_j} = \frac{\partial}{\partial x_j}\left[\left(\mu + \frac{\alpha \mu_t}{\sigma_k}\right) \frac{\partial k}{\partial x_j}\right] + L_{ij} \frac{\partial \tilde{u}_i}{\partial x_j} - \bar{\rho} \varepsilon, \tag{9}$$

$$\frac{\partial \bar{\rho} \varepsilon}{\partial t} + \frac{\partial \bar{\rho} \varepsilon \tilde{u}_j}{\partial x_j} = \frac{\partial}{\partial x_j}\left[\left(\mu + \frac{\alpha \mu_t}{\sigma_\varepsilon}\right) \frac{\partial \varepsilon}{\partial x_j}\right] + C_{\varepsilon 1}\left(\frac{\varepsilon}{k}\right) L_{ij} \frac{\partial \tilde{u}_i}{\partial x_j} - C_{\varepsilon 2} \bar{\rho} \frac{\varepsilon^2}{k}. \tag{10}$$

in which p is the pressure, σ_{ij} the viscous-stress tensor, μ the molecular viscosity, C_p the specific heat at constant pressure, T the temperature and Pr_t the turbulent Prandtl number. The following values have been used for the different parameters in the k and ε equations: $\sigma_\varepsilon = 1.4245$, $C_{\varepsilon 1} = 1.44$ and $C_{\varepsilon 2} = 11/6$.

Summarizing, wherever the LES SGS-viscosity is lower than the RANS eddy-viscosity ($\alpha < 1$), an expression very similar to the classical Smagorinsky model is obtained for the turbulent stresses by combining Eqs. (1), (3) and (4). The difference with the classical Smagorinsky model is the presence of the diagonal term proportional to k. However, for compressible flows, this can be considered as a model for the isotropic part of the SGS stresses. As discussed in Batten, *et al.* (2004), the model should work in the LES mode where the grid is fine enough to resolve a significant part of the turbulence scales, as in LES; elsewhere ($\alpha = 1$), the $k - \varepsilon$ RANS closure is recovered.

Note that in LNS R_{ij} is replaced with L_{ij} not only in the momentum and energy equations, but also in the two additional equations in k and ε. This implies that, although the total turbulent kinetic energy dissipates at the rate dictated by ε, the energy-production term $R_{ij} \frac{\partial \tilde{u}_i}{\partial x_j}$ is replaced by $L_{ij} \frac{\partial \tilde{u}_i}{\partial x_j} = \alpha R_{ij} \frac{\partial \tilde{u}_i}{\partial x_j}$. Consequently, a reduction of the turbulent kinetic energy production is obtained in those regions where a fraction of turbulence is directly simulated ($\alpha < 1$).

A reduction of the turbulent transport of k and ε in regions where $\alpha < 1$ is also obtained by replacing μ_t with $\alpha \mu_t$ in the RANS equations for k and ε.

Finally, one can notice that, by construction, the present version of the LNS model is no more time consuming than the RANS $k-\varepsilon$ model. Indeed, the extra-cost due to the evaluation of the Smagorinsky eddy viscosity is negligible compared to the overall computation required by the solution of the RANS $k-\varepsilon$ equations.

3. Numerical ingredients

The LES, RANS and LNS equations have been discretized in space using a mixed finite-volume/finite-element method applied to unstructured tetrahedrizations. The adopted scheme is vertex centered, i.e., all degrees of freedom are located at the vertices. P1 Galerkin finite elements are used to discretize the diffusive terms.

A dual finite-volume grid is obtained by building a cell C_i around each vertex i through the rule of medians. The convective fluxes are discretized on this tessellation, i.e., in terms of fluxes relative to the common boundaries shared by neighboring cells.

The Roe scheme (1981) represents the basic upwind component for the numerical evaluation of the convective fluxes $\mathcal{F}$:

$$\Phi^R(W_i, W_j, \vec{n}) = \frac{\mathcal{F}(W_i, \vec{n}) + \mathcal{F}(W_j, \vec{n})}{2} - \gamma_s\left[P^{-1}|P\mathcal{R}|\frac{W_j - W_i}{2}\right] \tag{11}$$

in which $\Phi^R(W_i, W_j, \vec{n})$ is the numerical approximation of the flux between the i-th and the j-th cells, W_i is the solution vector at the i-th node, $\vec{n}$ is the outward normal to the cell boundary and $\mathcal{R}(W_i, W_j, \vec{n})$ is the Roe Matrix. The matrix $P(W_i, W_j)$ is the Turkel-type preconditioning term, introduced to avoid accuracy problems at low Mach numbers (Guillard and Viozat 1999). Note that, since it only appears in the upwind part of the numerical fluxes, the scheme remains consistent in time and can thus be used for unsteady flow simulations. Finally, the parameter γ_s, which multiplies the upwind part of the scheme, collected within square brackets in Eq. (11), permits a direct control of the numerical viscosity, leading to a full upwind scheme for $\gamma_s = 1$ and to a centered scheme when $\gamma_s = 0$. The spatial accuracy of this scheme is only first order. The MUSCL linear reconstruction method ("Monotone Upwind Schemes for Conservation Laws"), introduced by van Leer (1977) is therefore employed to increase the order of accuracy of the Roe scheme. This is obtained by expressing the Roe flux between two cells, centered on two generic nodes i and j, as a function of the reconstructed values of W at their interface: $\Phi^R(W_{ij}, W_{ji}, \vec{n}_{ij})$, where W_{ij} is extrapolated from the values of W at nodes i and j. A reconstruction using a combination of different families of approximate gradients (P1-elementwise gradients and nodal gradients evaluated on different tetrahedra) is adopted, which allows a numerical dissipation made of sixth-order space derivatives to be obtained. The MUSCL reconstruction is described in detail in Camarri, *et al*. (2004), in which the capabilities of this scheme in concentrating the numerical viscosity effect on a narrow-band of the highest resolved frequencies is also discussed. As discussed in Camarri, *et al*. (2004), this is specially important in LES simulations to limit as far as possible the interactions between numerical and SGS dissipation, which could deteriorate the accuracy of the results.

Either implicit or explicit schemes can be used to advance the equations in time by a line method, i.e., time and space are treated separately. In the explicit case a N-stage low-storage Runge-Kutta algorithm is available, in which the number of stages and the coefficients can be varied to obtain different schemes. An implicit time marching algorithm is also available in the code, based on a second-order time-accurate backward difference scheme. A first-order semi-discretization of the jacobians is used together with a defect-correction procedure (Martin and Guillard 1996); the resulting scheme is linearly unconditionally stable and second-order accurate.

More details on the numerical ingredients used in the present work can be found in Camarri, *et al.* (2002a), Farhat, *et al.* (1999).

4. Test-case description and simulations parameters

The flow around a square cylinder of infinite length is considered. The Reynolds number, based on the cylinder side length and on the freestream velocity, is equal to 22000 and the used computational domain is represented in Fig. 1, together with the frame of reference.

In the first set of simulations, with reference to Fig. 1, the domain dimensions are the following: $L_i/D=4.5$, $L_0/D=9.5$, $H_y/D=7$, $H_z/D=4$. They are equal to those employed by contributors to the LES workshop (Rodi, *et al.* 1997), except for a shorter distance between the cylinder and the inflow boundary L_i. The computational domain in Fig. 1 is discretized by generating an unstructured grid made of 97980 nodes and 559136 tetrahedral elements (grid GR1 in Table 1). The section $z=0$ of

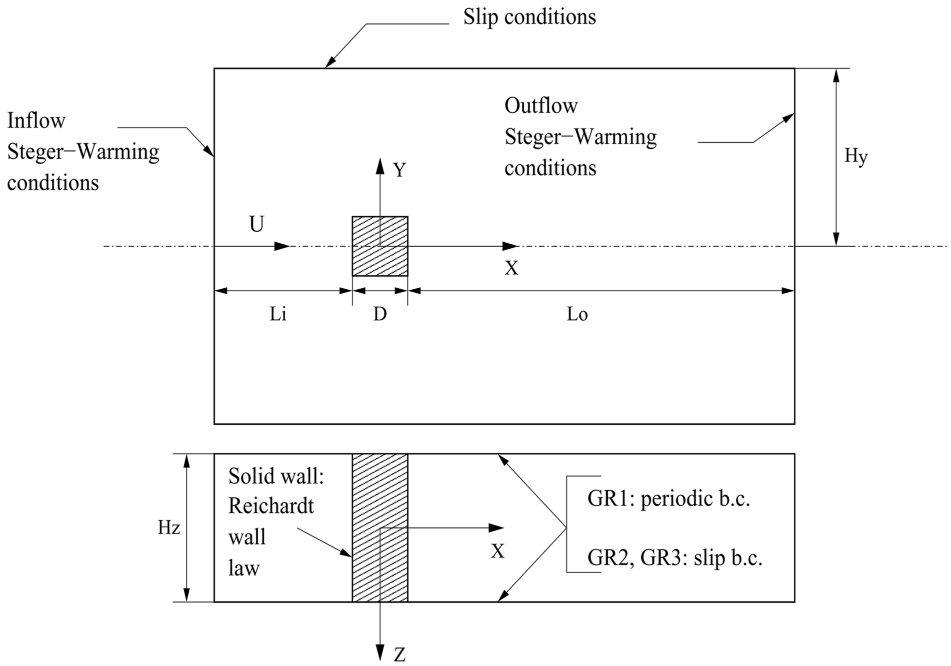

Fig. 1 Computational domain and frame of reference

Table 1 Main feature of the computational domains and grids

Grid	L_i/D	L_0/D	H_y/D	H_z/D	Nodes	Elements	δ/D
GR1	4.5	9.5	7	4	9.8×10^4	5.6×10^5	0.06
GR2	4.5	9.5	7	9.75	8.3×10^4	4.57×10^5	0.06
GR3	4.5	9.5	7	9.75	3.5×10^4	1.9×10^5	0.07

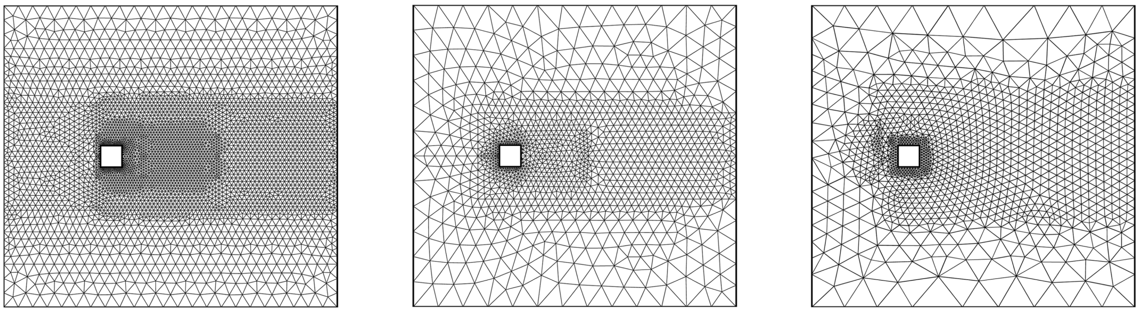

(a) (b) (c)

Fig. 2 Computational grids; section at z=0. (a) GR1; (b) GR2; (c) GR3

the grid is reported in Fig. 2(a).

Approximate boundary conditions, based on the Reichardt wall-law (Hinze 1959, Mohammadi and Pironneau 1997), are applied at the solid walls. This law has the advantage of describing the velocity profile not only in the logarithmic region of a boundary layer but also in the laminar sublayer and in the intermediate region. This type of wall treatment has been successfully used in previous LES (Camarri, *et al*. 2002b, Camarri, *et al*. 2004, Koobus and Farhat 2004) and RANS (Mohammadi and Pironneau 1997, Mohammadi and Medic 1998) simulations of the same flow. Finally, this approach allows the same boundary conditions to be used for both the RANS closure and the LES Smagorinsky model. At the inflow, the flow is assumed to be undisturbed and the Steger-Warming (1981) conditions are applied. Boundary conditions based on the Steger-Warming decomposition are used at the outflow as well. On the top and bottom surfaces ($y=\pm H_y$) slip conditions are imposed. Finally, the flow is assumed to be periodic in the spanwise direction in order to simulate a cylinder of infinite spanwise length.

The grid GR1 has an LES-like resolution and was already used for the LES simulations documented in Camarri, *et al*. (2004), Camarri, *et al*. (2002b); thus, as already stated in the Introduction, this first set of simulations is aimed to verify whether the LNS approach actually tends to LES for fine grids.

Conversely, the second and third sets of simulations are aimed to investigate the capabilities of the LNS approach in cases in which it should work in a hybrid mode. In these simulations, a different computational domain and coarser grids are used. In particular, the new domain has been extended in the spanwise direction, i.e., $H_z/D=9.75$, while the other dimensions are kept unchanged. The spanwise extension of the new domain is the same as that of the water tunnel used in the experiments of (Lyn, *et al*. 1995, Lyn and Rodi 1994). Thus, in the second and third sets of simulations, slip conditions have been applied also in the spanwise direction instead of periodic ones. The remaining boundary conditions are unchanged. The main features of the grids employed in the second and third set of simulations (GR2 and GR3 respectively) are reported in Table 1. A horizontal cut of GR2 and GR3 is shown in Figs. 2(b) and 2(c), respectively.

In all cases, three computations have been carried out, using respectively the LES approach with the Smagorinsky SGS model, the RANS $k-\varepsilon$ closure and the LNS model.

Following the sensitivity studies in Camarri, *et al*. (2004), Camarri, *et al*. (2002b), for each set of computations the numerical parameter γ_s, which controls the amount of numerical viscosity introduced in the simulation, has been set equal to the smallest value needed to obtain a stable LES simulation. Note that, as mentioned in Sec. 3 and shown in Camarri, *et al*. (2004), in the present approach, the numerical viscosity only acts on a narrow band of the highest resolved frequencies.

Moreover, it has been shown in Camarri, *et al*. (2004) that with the present approach a very fine tuning of the γ_s parameter is not needed in order to obtain reliable results, provided that the value of γ_s is maintained significantly lower than 1.

As for preconditioning, a preliminary study (not reported here for sake of brevity) has shown that for grids GR1 and GR2 the results are not sensitive to preconditioning, while for GR3 it was needed to avoid accuracy problems in the vicinity of the stagnation point.

The simulations on grid GR1 are advanced in time using an explicit 4 steps Runge-Kutta scheme. Conversely, the simulations carried out on grids GR2 and GR3 have been implicitly advanced in time, with a maximum CFL number equal to 25. In our simulations the CFL is multiplicative factor, so that for each node of the computational grid the time step is defined as the maximum local time step allowed by the stability of the explicit Runge-Kutta 1 scheme multiplied by CFL. Since the simulations are unsteady, the actually used Δt is the same for all nodes (equal to the minimum of the local time steps). With this time step, about 130 time iterations per shedding cycles are used. The maximum CFL number has been selected according to the following criterion. It has been verified that the time step Δt corresponding to the selected CFL number was small enough in order to satisfy the following inequality in the whole computational domain:

$$V_i \Delta T \leq \Delta L.$$

where V_i denotes the modulus of the velocity on the i-th node and ΔL is a length representative of the local grid resolution (in our case the average length among the edges attached to the node). Although we have already applied this criterion with success in other simulations (see Camarri, *et al*. 2004), we have a-posteriori checked that, using CFL=25 with the implicit algorithm, no significant information is lost in time with respect to the case of the Runge-Kutta scheme with CFL=1 (see Appendix 1).

5. Results and discussion

5.1. Bulk coefficients and time-averaged flow field

The present flow configuration has been the object of a large amount of simulations (see, for instance, the review papers (Rodi, *et al*. 1997, Voke 1997 and Rodi 2002). The bulk coefficients obtained in the simulations on grid GR1 are reported in Table 2, together with some examples of results obtained with different numerical approaches, and namely with DES (Schmidt and Thiele 2002), LES (Fureby, *et al*. 2000, Rodi, *et al*. 1997, Sohankar, *et al*. 2000) and RANS simulations (Bosh and Rodi 1998) as well as the experimental data from Lyn, *et al*. (1995), Lyn and Rodi (1994), Bearman and Obasaju (1982). The values in the brackets in Table 2 (as also for Table 3 in the following) indicate the range of values obtained for each of the considered parameters in the different simulations presented in the cited references. Concerning Bosh and Rodi (1998), we have considered only those simulations that have been carried out using the standard $k-\varepsilon$ model on a computational domain having the same distance between the cylinder and the inflow boundary as the one adopted here. The frequency of the vortex shedding f_s is reported in Table 2 in terms of Strouhal number $St=f_sD/U_\infty$, U_∞ being the free-stream velocity.

The results summarized in Table 2 confirm that the LNS approach actually tends to LES when the grid in refined enough. Indeed, while the $k-\varepsilon$ model gives predictions that are far from the experiments, the LNS predicts the bulk coefficients with almost the same accuracy as the LES Smagorinsky model. A detailed comparison between our LES results and both the experimental data

Table 2 Bulk coefficients: numerical results obtained in the simulations carried out on grid GR1 together with experimental data and with other simulations described in the literature

Simulations	C'_l	$\overline{C_d}$	C'_d	S_t	l_r
RANS (present)	0.62	1.64	0.02	0.134	2.14
LES (present)	0.84	1.89	0.09	0.132	1.41
LNS (present)	0.87	1.91	0.10	0.134	1.50
DES (Schmidt and Thiele 2002)	[1.36,1.55]	[2.42,2.57]	[0.28,0.68]	[0.09,0.13]	[1.16,1.37]
LES (Rodi, *et al*. 1997)	[0.38,1. 79]	[1.66,2.77]	[0.10,0.27]	[0.07,0.15]	[0.89,2.96]
LES (Sohankar, *et al*. 2000)	[1.23,1.54]	[2.03,2.32]	[0.16,0.20]	[0.127,0.132]	---
LES (Fureby, *et al*. 2000)	[1.30,1.34]	[2.0,2.2]	[0.17,0.20]	[0.129,0.135]	[1.29,1.34]
RANS (Bosh and Rodi 1998)	[0.05,0.40]	[1.62,1.83]	[0.0003,0.0057]	[0.126,0.140]	---
EXP. (Lyn and Rodi 1994)	---	2.1	---	0.132±0.004	1.4
EXP. (Bearman and Obasaju 1982)	1.2	2.28	---	0.130	---

$\overline{C_d}$ is the mean drag coefficient, C'_d and C'_l are the r.m.s. of the drag and lift coefficients, S_t is the Strouhal number and l_r is the length of the mean recirculation bubble.

and the results of the other simulations cited in Table 2 was already carried out in Camarri, *et al.* (2002b), and is not repeated here for sake of brevity. The convergence of the LNS approach to the Smagorinsky model on GR1 is also clear from the visualization of α within the domain; indeed, in this case the LNS model works in LES model almost everywhere. A more detailed discussion of this point is carried out in Sec. 5.2.

The bulk coefficients obtained with the different turbulence models on grids GR2 and GR3 are shown in Table 3, together with the same DES, LES, RANS and experimental results also reported in Table 2.

Although the number of nodes of GR2 is not significantly lower than that of GR1, note that they

Table 3 Bulk coefficients: numerical results obtained in the simulations carried out on grids GR2 and GR3 together with experimental data and with other simulations described in the literature

Simulations	C'_l	$\overline{C_d}$	C'_d	S_t	l_r
RANS (present, GR2)	0.96	1.77	0.0712	0.1340	2.05
LES (present, GR2)	1.15	2.05	0.197	0.120	1.27
LNS (present, GR2)	1.0	2.0	0.155	0.127	1.29
RANS (present, GR3)	0.20	1.53	0.01	0.117	2.38
LES (present, GR3)	0.31	1.71	0.02	0.137	2.80
LNS (present, GR3)	0.77	1.93	0.07	0.128	1.46
DES (Schmidt and Thiele 2002)	[1.36,1.55]	[2.42,2.57]	[0.28,0.68]	[0.09,0.13]	[1.16,1.37]
LES (Rodi, *et al*. 1997)	[0.38,1. 79]	[1.66,2.77]	[0.10,0.27]	[0.07,0.15]	[0.89,2.96]
LES (Sohankar, *et al*. 2000)	[1.23,1.54]	[2.03,2.32]	[0.16,0.20]	[0.127,0.132]	---
LES (Fureby, *et al*. 2000)	[1.30,1.34]	[2.0,2.2]	[0.17,0.20]	[0.129,0.135]	[1.29,1.34]
RANS (Bosh and Rodi 1998)	[0.05,0.40]	[1.62,1.83]	[0.0003,0.0057]	[0.126,0.140]	---
EXP. (Lyn and Rodi 1994)	---	2.1	---	0.132±0.004	1.4
EXP. (Bearman and Obasaju 1982)	1.2	2.28	---	0.130	---

$\overline{C_d}$ is the mean drag coefficient, C'_d and C'_l are the r.m.s. of the drag and lift coefficients, S_t is the Strouhal number and l_r is the length of the mean recirculation bubble.

are distributed in a computational domain that is 2.4 times larger than for GR1; thus, the resolution of GR2 was not a priori expected to be adequate for LES. However, the agreement of the LES bulk coefficients with the experimental ones is still quite satisfactory and, surprisingly, some of them, as the mean drag coefficient or the C_l r.m.s., are even better predicted than with GR1. The reason of this behavior might be twofold. First, in the computations with GR2, no periodicity is imposed in the spanwise direction, but all the extent of the experimental model is taken into account, and, thus, the spanwise length of the 3D structures is not a-priori imposed, as is implicitly done in the computations with GR1. Moreover, due to the difficulty in precisely controlling the quality of unstructured grids, it appears that GR2, in spite of its coarser resolution, is more regular near the body than GR1, which has problems in the region immediately upstream of the stagnation point (see Sec. 5.2 and Figs. 2a and 2b), and this could also lead to an improvement of the force prediction. As for GR1, the differences between the results obtained with LNS and those given by LES on GR2 are rather small, as shown, for bulk coefficients, in Table 3. The same is observed also for the averaged velocity fields (not shown here). Indeed, for this grid resolution, where the closure term is significant, the LNS simulation works in the LES mode, except for a small zone around the upwind corners of the cylinder. We refer again to Sec. 5.2 for more details.

Grid GR3 has definitely a very low resolution, compared with all the other LES or hybrid simulations reported in the literarture. Although the comparison is not completely meaningful since our domain is larger and our grids are unstructured, note that the LES in Fureby, *et al.* (2000), Sohankar, *et al.* (2000) have been carried out on grids with a number of nodes between 10 and 20 times larger than in grid GR3, and the DES simulations in (Schmidt and Thiele 2002) have been carried out with a number of nodes varying from 6×10^4 to 6×10^5. Indeed, on GR3 the Smagorinsky model leads, as expected, to rather inaccurate predictions of the bulk coefficients. On the other hand, also the $k-\varepsilon$ model gives a poor prediction of the force coefficients, although results are still comparable with those in (Bosh and Rodi 1998). Moreover, in both LES and RANS simulations, the remarkable underestimate of C'_l and C'_d indicates problems in the correct prediction of the vortex shedding, which are confirmed also by the errors observed for the drag coefficient. Table 3 shows that the LNS approach improves noticeably the results with respect to the $k-\varepsilon$ and the Smagorinsky models. In particular, the drag coefficient is predicted with an error of about 9%, which might be acceptable in some engineering applications and which is even more accurate than some LES described in the literature (see Rodi, *et al.* 1997). The values of C'_l and C'_d, although underestimated with respect to the experiments, indicate that the vortex shedding is predicted without the difficulties encountered by the RANS and the LES models. In particular, by analyzing the time history of the lift coefficients obtained in the different simulations, reported together for a representative time interval in Fig. 3, it is clear that the $k-\varepsilon$ model predicts a periodic behavior for the lift coefficient, with an amplitude of the oscillations lower than the experimental value, as shown in Table 3. Although the r.m.s. of the lift coefficient is still severely underestimated with the Smagorinsky model, a more realistic modulation in the amplitude of the oscillations is observed. Finally, the LNS simulation predicts a lift coefficient which shows the experimentally-observed modulations in amplitude, as with the Smagorinsky model, but the r.m.s. of the coefficient is definitely larger and closer to the experimental value than for the previous two cases.

This indicates that in the LNS simulation the time fluctuations of the different quantities are less damped than in the LES and RANS ones. This aspect is even more evident when the instantaneous velocity field is considered, as shown for instance in Fig. 4, where the time

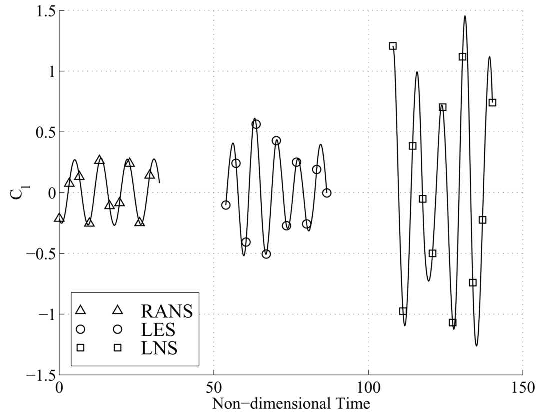

Fig. 3 Lift coefficient obtained in the simulations carried out on grid GR3

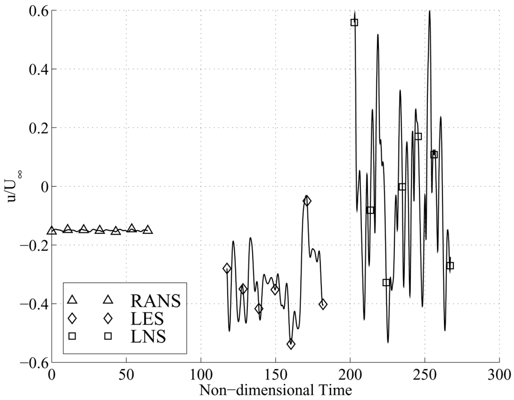

(a) u/U_∞

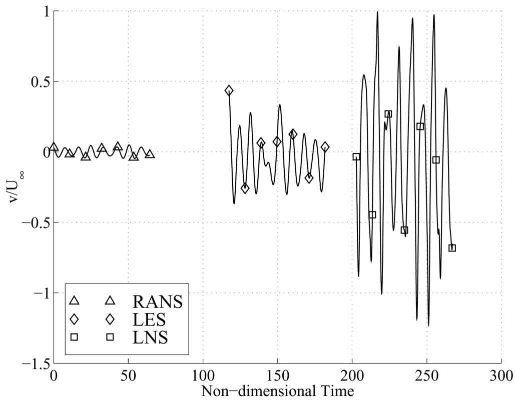

(b) v/U_∞

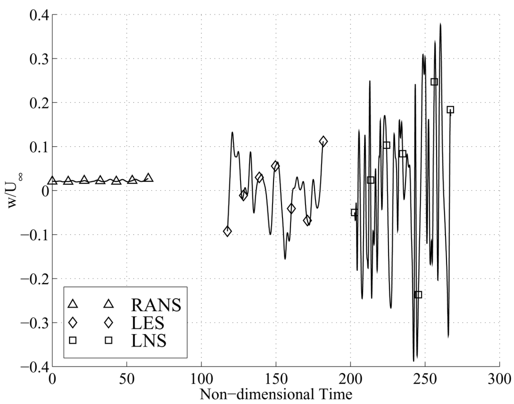

(c) w/U_∞

Fig. 4 Instantaneous velocity obtained on grid GR3 at the point of coordinates x=1, y=0, z=0 behavior of the velocity components obtained in the simulations on grid GR3 is plotted for a point within the wake. In particular, Fig. 4(c), in which the velocity fluctuations in the spanwise direction are reported, well underlines the capabilities of the LNS approach in the description of the flow three-dimensional fluctuations that are almost absent in the RANS approach and damped in the LES one. Moreover, it can be noticed that signals from LNS contain higher frequencies in time with respect to the other two approaches and this might also indicate that small scales are less damped in LNS.

Finally, the values of the recirculation length in Table 3 indicate that the LNS approach also improves the description of the time-averaged flow field. This is confirmed in Fig. 5a, where the profiles of the mean streamwise velocity obtained on the centerline of GR3 are reported for the three different approaches and compared with the experimental data. Indeed, in the near wake the mean velocity profile obtained through the LNS approach agrees rather well with the experimental data, while both LES and RANS gives completely wrong predictions. More downstream, the recovery of the streamwise velocity is significantly overestimated in the LNS simulation. However,

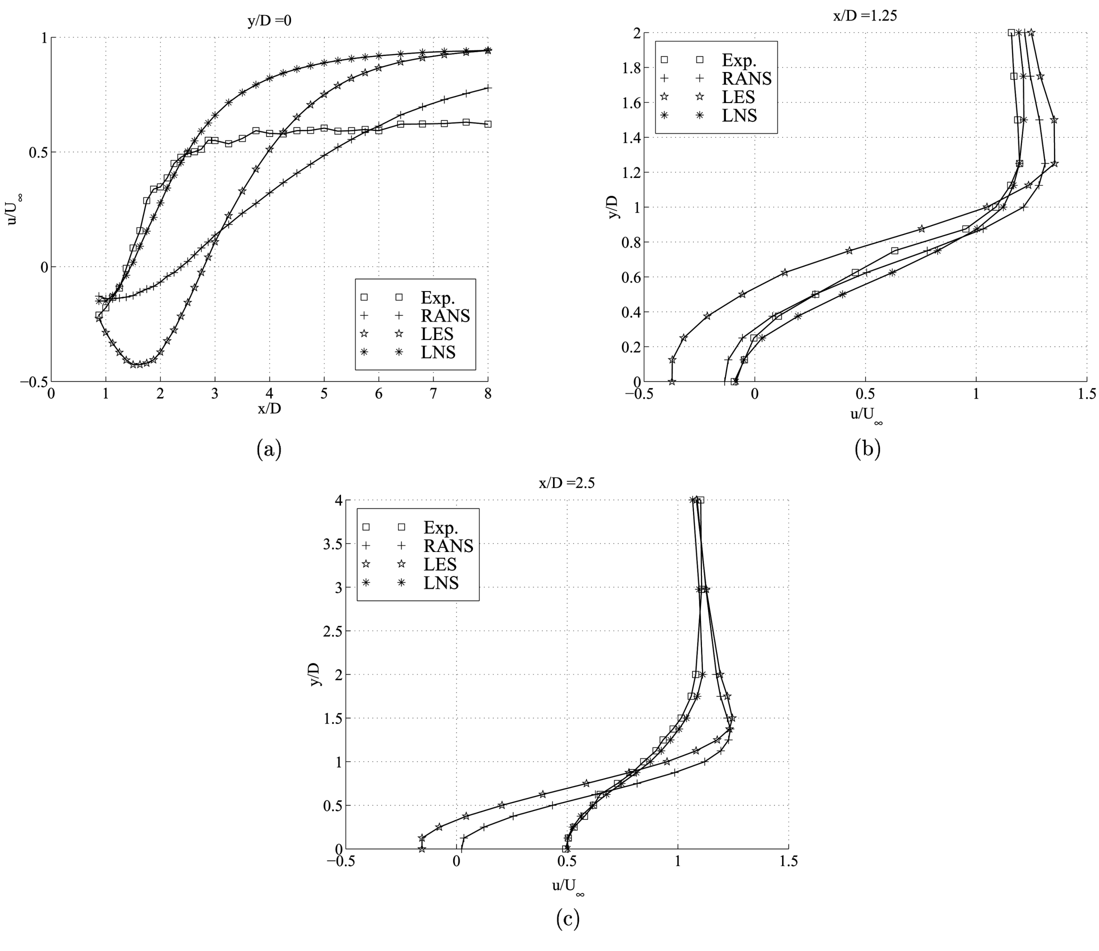

Fig. 5 Time averaged streamwise velocity obtained on grid GR3 on the centerline (a) and at vertical sections *x/D*=1.25 (b) and *x/D*=2.5 (c) (*z*=0); experimental data are taken from (Lyn, *et al*. 1995)

this problem was also observed in the LES simulations on the most refined grid (see Camarri, *et al*. 2002b) and is common to other large-eddy simulations in the literature (see, for instance, Bosh and Rodi 1998, Sohankar, *et al*. 2000, Fureby, *et al*. 2000). Finally, Figs. 5(b) and 5(c) show the mean streamwise velocity obtained on GR3 at two vertical sections in the wake; again, the best agreement with the experimental data is obtained with the LNS approach.

Summarizing, as expected, the results obtained with the $k-\varepsilon$ RANS model are not satisfactory for all the considered grid resolutions, while LES gives good predictions for the most refined grids, but the quality of the results is very sensitive to the grid resolution, leading to unacceptable predictions on the coarsest grid. Conversely, at least for the considered flow, the LNS approach recovers the LES accuracy on fine grids, but also reduces and almost eliminates the sensitivity to grid resolution, giving acceptable results also on the coarsest grid. This suggests that LNS may give satisfactory predictions in the simulation of higher Reynolds number flows, for which only coarse grid resolutions may be used due to practical limitations of computational resources.

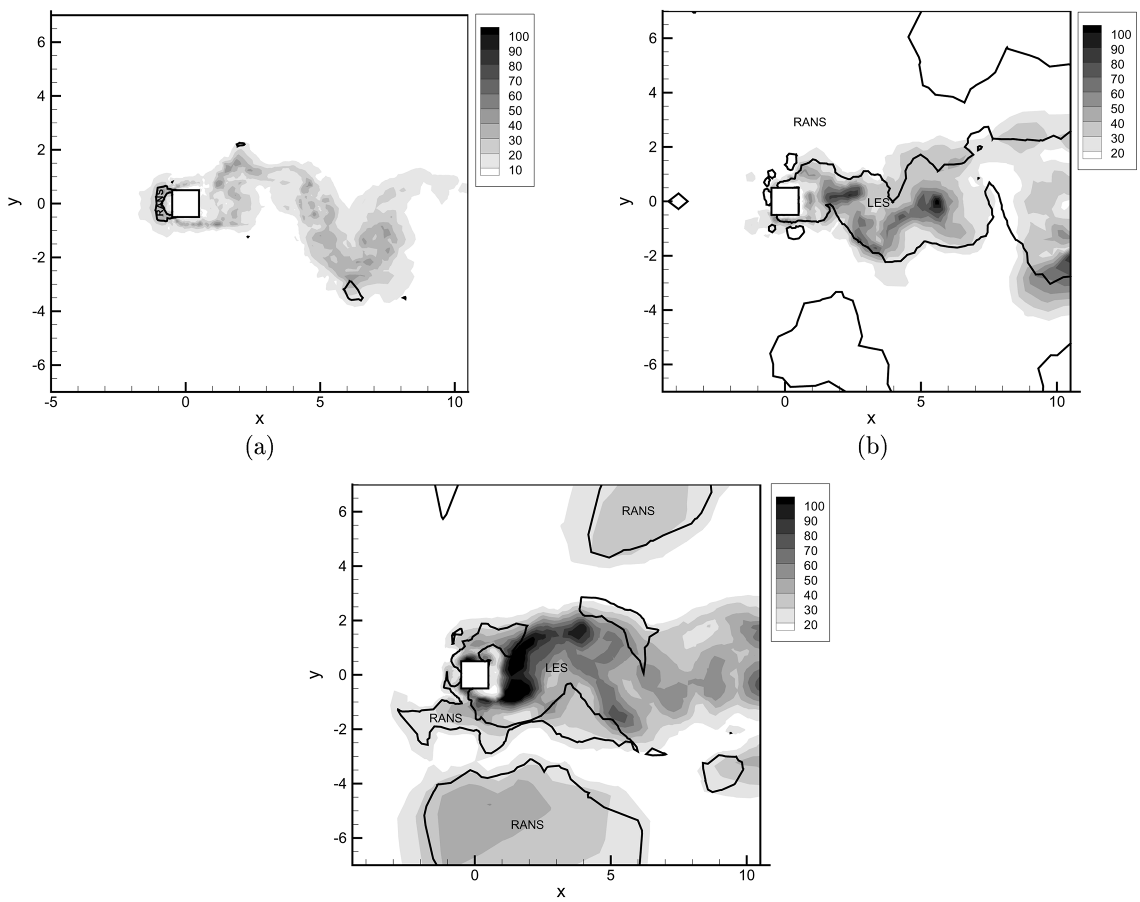

Fig. 6 Instantaneous contours of the LES eddy-viscosity for the LNS simulations on grids GR1 (a), GR2 (b) and GR3 (c); plane z=0. The considered time instants correspond to a peak (positive or negative) in the time history of the C_l coefficient

5.2. Eddy-viscosity fields obtained in the LNS simulations

Let us analyze now in more detail how the Smagorinsky and $k-\varepsilon$ eddy viscosities are blended together in LNS. The instantaneous values of the LES eddy-viscosity obtained in the LNS simulations on the plane $z=0$ of GR1, GR2 and GR3 are visualized in Fig. 6. The isoline corresponding to $\alpha=0.95$ is also reported as a numerical threshold between the zones in which the LNS model works in LES or RANS modes. Although Figs. 6 show instantaneous situations, they are representative of the typical behavior throughout the simulation.

For all the grid resolutions, the LNS model works in the LES mode within the wake and this is a positive feature since it is anticipated that RANS closures are too dissipative for unsteady separated wakes. This is also in agreement with the behavior of other hybrid approaches, as, for instance, DES.

The situation is more complex near the body. From a general viewpoint, it may be observed that the RANS mode is used whenever the velocity gradients in the flow and the grid resolution are such that the subgrid eddy-viscosity given by the Smagorinsky model becomes very high (see Eq. 5) and remember that in our formulation the filter width depends on the grid size). This behavior is evident for instance, for the finest grid, for which the RANS model is only used in a small region upstream of the stagnation point, in which velocity gradients are obviously high and the grid is not very well designed (see Fig. 2a). On the coarsest grid (Fig. 6c), the grid resolution is such that the RANS closure is active on most of the upwind edge of the cylinder. However, Fig. 6(c) also shows that, in proximity of the stagnation point, the Reynolds stress tensor is damped, i.e., the LES eddy-viscosity is used. This may again be considered a positive feature, because a known drawback of the standard k-ε model is the excessive eddy-viscosity introduced at the stagnation point. The LNS simulation works in the RANS mode also in the shear-layers detaching from the cylinder. This is probably the key point which leads to the improvement of the results obtained with LNS compared to those given by LES on this grid, as described in Sec. 5.1.

The observed behavior of LNS is not completely in agreement with the rationale of most of the hybrid approaches, which is to use RANS near the body. However, the present results can not be considered, in our opinion, as a final assessment of the near-body behavior of LNS for two main reasons. The first one is that the employed grids are nearly isotropic near the wall, and not highly stretched as usually done in RANS or in other hybrid calculations. We did not use highly stretched grids, because our numerical method in its present implementation is not accurate on highly stretched grids. Modifications of the construction of the finite-volume cells are in progress and new calculations on more stretched grids are forthcoming. Moreover, the classical $k-\varepsilon$ model has been used with no ad-hoc treatment near the wall, which could lead to too high a RANS eddy-viscosity in this region. The behavior of LNS with different RANS closures is another point to be investigated.

Finally, Fig. 6(c) shows that significant values of the SGS viscosity are given by the Smagorinsky model in some regions outside the wake near the lateral boundaries, in which the flow should be laminar. This is a typical problem encountered by the Smagorinsky model when the grid resolution is very coarse and is relevant to unstructured grids, in which very large elements can be used in the far-field (see, e.g., Camarri, *et al*. 2002b). Fig. 6(c) also shows that this problem is overcome in LNS by switching to the RANS mode.

6. Conclusions

A hybrid RANS/LES method based on the LNS concept has been applied to the numerical simulation of a classical benchmark for bluff-body flows, i.e., the flow around an infinite-length square cylinder at $Re = 22000$.

The basic ingredients of the LNS approach are a SGS model, a RANS closure model and a blending parameter, based on the values of the eddy viscosities given by the SGS and RANS closures. In our formulation, the SGS model is the one proposed by Smagorinsky while the RANS closure is given by the classical $k-\varepsilon$ approach.

The numerical discretization is based on a second order accurate mixed finite-element/finite-volume method, applied to unstructured tetrahedral grids. It uses a sophisticated MUSCL reconstruction leading to a numerical viscosity made of sixth-order spatial derivatives. Either an explicit Runge-Kutta algorithm or a second-order time-accurate implicit scheme can be used to advance the equations in time.

Simulations carried out on a grid sufficiently refined for LES have shown that, as anticipated, the LNS results are almost identical to those given by LES when the grid resolution is adequate. As also expected, the RANS approach with the $k-\varepsilon$ model gives poor results also on this refined grid. Note that the standard $k-\varepsilon$ model has been used, although it is known that it has significant difficulties in predicting bluff-body flows, in order to study the capabilities of the LNS approach with the most common RANS closure available in engineering codes and in an unfavorable situation.

More interestingly, when a significantly coarser grid is used, the LNS is able to describe the unsteadiness of the flow related to large structures, such as the vortex shedding from the cylinder, while both the LES and the RANS approaches introduce a too large eddy-viscosity and lead to an excessive damping of the flow unsteadiness. Moreover, the agreement with experimental data obtained with LNS is still acceptable and comparable to that of LES simulations in the literature, carried out on much more refined grids.

An a-posteriori analysis has also shown that the LNS blending criterion, although empirically based, leads to a sensible behavior, at least for the present test-case. Indeed, for all the grid resolutions, the LNS model works in LES mode in the separated unsteady wake, and this is consistent with the rationale of hybrid models. On the coarsest grid, the RANS closure is also used on the upwind cylinder face, except near the stagnation point, where, however, the standard $k-\varepsilon$ closure is known to give a too large eddy-viscosity. Moreover, for the coarsest grid, the RANS mode is used also in the detaching shear layers, thus damping the very high viscosity given by the Smagorinsky model due to the coarse resolution; this is probably the key point leading to an improvement of the results. However, the near wall behavior of the LNS model needs further investigation, and namely on more stretched grids and with more accurate RANS closures.

Finally, it has also been shown that implicit time advancing, which allows large time steps to be used, is very convenient for this kind of simulations, leading to noticeably less CPU consuming simulations without loosing any information on the results.

Acknowledgements

The simulations presented in this work were performed using the computational facilities of CINECA (Italy), whose support is gratefully acknowledged.

References

Alabakin, I., Braza, M., Camarri, S., Dervieux, A., Koobus, B., Kozubskaya, T., Rodes, P. and Salvetti, M.V. (2003), "Unstable and unsteady aerodynamics: compared information from different numerical models", In

Périaux, J., Champion, M., Gagnepain, J.-J., Pironeeau, O., Stoufflet, B. and Thomas, P., *Fluid Dynamics and Aeroacoustics: new challenges*, pp. 253-277, CIMNE, Barcelona.

Bagget, J.S., Jiménez, J. and Kravchenko, A.G. (1997), "Resolution requirements in large-eddy simulations of shear flows", Annual Research Briefs, Center for Turbulence Research, Stanford (CA), 51-66.

Batten, P. (2002), "LNS-An approach towards embedded LES", *AIAA Paper 2002-0427*. American Institute of Aeronautics and Astronautics.

Batten, P., Goldberg, U. and Chakravarthy, S. (2004), "Interfacing statistical turbulence closures with large-eddy simulation", *AIAA J.*, **42**(3), 485-492.

Batten, P., Goldberg, U.C., Palaniswamy, S. and Chakravarthy, S.R. (2001), "Hybrid LES-RANS: spatial-resolution and energy-transfer issues", In Lindborg, E., Johansson, A., Eaton, J., Humphrey, J., Kasagi, N. Leschziner, M. and Sommerfeld, M. Eds., *Turbulence and shear flow phenomena*, vol. 2, 159-164. KTH, Universitetsservice US AB.

Bearman, P.W. and Obasaju, E.D. (1982), "An experimental study of pressure fluctuations on fixed and oscillating square-section cylinders", *J. Fluid Mech*., **119**, 297-321.

Bosh, G. and Rodi, W. (1998), "Simulation of vortex shedding past a square cylinder with different turbulence models", *Int. J. Num. Meth. Fluids*, **28**, 601-616.

Breuer, M., Jovicic, N. and Mazaev, K. (2003), "Comparison of DES, RANS and LES for the separated flow around a flat plate at high incidence", *Int. J. Num. Meth. Fluids*, **41**, 357-388.

Camarri, S., Koobus, B., Salvetti, M.V. and Dervieux, A. (2002a), "A low diffusion MUSCL scheme for LES on unstructured grids", *Technical Report RR-4512*, INRIA.

Camarri, S., Salvetti, M.V., Koobus, B. and Dervieux, A. (2002b), "Large-eddy simulation of a bluff-body flow on unstructured grids", *Int. J. Num. Meth. Fluids*, **40**, 1431-1460.

Camarri, S., Salvetti, M.V., Koobus, B. and Dervieux, A. (2004), "A low diffusion MUSCL scheme for LES on unstructured grids", *Computers & Fluids*, **33**, 1101-1129.

Constantinescu, G.S., Pasinato, H., Wang, Y.Q., Forsythe, J.R. and Squires, K.D. (2002), "Numerical investigation of flow past a prolate spheroid", *ASME J. Fluids Eng.*, **124**, 904-910.

Constantinescu, G.S. and Squires, K.D. (2003), "LES and DES investigations of turbulent flow over a sphere at *Re*=10000", *Flow, Turbulence and Combustion*, **70**, 267-298.

Durbin, P.A. (1995), "Separated flow computations with the k-ε-v^2 model", *AIAA J.*, **33**(4), 659-664.

Farhat, C., Koobus, B. and Tran, H. (1999), "Simulation of vortex shedding dominated flows past rigid and flexible structures", In *Computational Methods for Fluid-Structure Interaction*, pp. 1-30, Tapir.

Fureby, C., Tabor, G., Weller, H.G. and Gosman, A.D. (2000), "Large eddy simulation of the flow around a square prism", *AIAA J.*, **38**(3), 442-452.

Guillard, H. and Viozat, C. (1999), "On the behaviour of upwind schemes in the low Mach number limit", *Computers & Fluids*, **28**, 63-86.

Hedges, L.S., Travin, A.K. and Spalart, P.R. (2002), "Detached-eddy simulation of a simplified landing gear", *ASME J. Fluids Eng.*, **124**, 413-423.

Hinze, J. (1959), *Turbulence*. MacGraw-Hill, New York.

Kato, M. and Launder, B.E. (1993), "The modelling of turbulent flow around stationary and vibrating square cylinders", In *Proc. 9th Symp. Turbulent Shear Flows*.

Koobus, B. and Farhat, C. (2004), "A variational multiscale method for the large eddy simulation of compressible trurbulent flows on unstructured meshes-application to vortex shedding", *Comput. Methods Appl. Mech. Eng.*, **193**, 1367-1383.

Koobus, B., Fahrat, C. and Tran, H. (2000), "Computation of unsteady viscous flows around moving bodies using the k-ε turbulence model on unstructured dynamic grids", *Comput. Methods Appl. Mech. Eng.*, **190**(11-12), 1441-1466.

Kotapati-Apparao, R.B and Squires, K.D. (2003), "Prediction of a prolate spheroid undergoing a pitchup maneuver", *AIAA Paper 2002-0269*, Reno, NV. American Institute of Aeronautics and Astronautics.

Lakehal, D. and Thiele, F. (2001), "Sensitivity of turbulent shedding flows to non-linear stress-strain relations and Reynolds stress models", *Comput. Fluids*, **30**, 1-35.

Launder, B. and Spalding, D. (1979), "The numerical computation of turbulent flows", *Comp. Meth. Appl. Mech. and Eng.*, **3**, 269-289.

Lenormand, E., Sagaut, P. and Phuoc, L.T. (2000), "Large eddy simulation of subsonic and supersonic channel flow at moderate Reynolds number", *Int. J. Num. Meth. Fluids*, **32**, 369-406.
Lubke, H., Schmidt, S., Rung, T. and Thiele, F. (2001), "Comparison of LES and RANS in bluff-body flows", *J. Wind Eng. Ind. Aerodyn.*, **89**, 1471-1485.
Lyn, D.A., Einav, S., Rodi, W. and Park, J.H. (1995), "A laser-doppler velocimeter study of ensemble-averaged characteristics of the turbulent near wake of a square cylinder", *J. Fluid Mech.*, **304**, 285-319.
Lyn, D.A. and Rodi, W. (1994), "The flapping shear layer formed by flow separation from the forward corner of a square cylinder", *J. Fluid Mech.*, **267**, 353-376.
Martin, R. and Guillard, H. (1996), "A second order defect correction scheme for unsteady problems", *Computers & Fluids*, **25**(1), 9-27.
Menter, F.R. (1993), "Zonal two-equation k-ω turbulence models for aerodynamic flows", *Technical Report 93-2906*, American Institute of Aeronautics and Astronautics.
Mohammadi, B. and Medic, G. (1998), "A critical evaluation of the classical k-epsilon model and wall-laws for unsteady flows over bluff bodies", *Int. J. Comp. Fluid Dyn.*, **10**(1), 1-11.
Mohammadi, B. and Pironneau, O. (1997), "Unsteady separated turbulent flows computation with wall-laws and k-ε model", *Comput. Method Appl. M.*, **148**(3-4), 393-405.
Omari, K.E., Schall, E., Koobus, B. and Dervieux, A. (2003), "Turbulence modeling challenges in airship studies", In del Galdeano, G., de Silanes, L. and *et al*., editors, *Monografias del Seminario Matematico*, pp. 545-554.
Rodi, W. (2002), "Large eddy simulations of the flow past bluff bodies", In Launder, B. and Sandham, N., editors, *Closure Strategies for Turbulent and Transitional Flows*, pp. 361-391. Cambridge University Press.
Rodi, W., Ferziger, J.H., Breuer, M. and Pourquié, M. (1997), "Status of large eddy simulation: results of a workshop", *ASME J. Fluids Eng.*, **119**, 248-262.
Roe, P.L. (1981), "Approximate Riemann solvers, parameters, vectors and difference schemes", *J. Comp. Phys*., **43**, 357-372.
Schmidt, S. and Thiele, F. (2002), "Comparison of numerical methods applied to the flow over wall-mounted cubes", *Int. J. of Heat and Fluid Flow*, **23**, 330-339.
Shur, M., Spalart, P.R., Strelets, M. and Travin, A. (1999), "Detached-eddy simulation of an airfoil at high angle of attack", In Rodi, W. and Laurence, D., editors, *Engineering Turbulence Modelling and Experiments-4.* Elsevier Science.
Smagorinsky, J. (1963), "General circulation experiments with the primitive equations", *Monthly Weather Review*, **91**(3), 99-164.
Sohankar, A., Davidson, L. and Norberg, C. (2000), "Large eddy simulation of flow past a square cylinder: comparison of different subgrid scale models", *ASME J. Fluids Eng.*, **122**, 39-47.
Spalart, P.R. and Allmaras, S.R. (1994), "A one-equation turbulence model for aerodynamic flows", *La Recherche Aérospatiale*, **1**, 5-21.
Spalart, P.R., Jou, W.H., Strelets, M. and Allmaras, S. (1997), "Comments on the feasibility of LES for wings and on a hybrid RANS/LES approach", In Liu, C. and Liu, Z., editors, *Advances in DNS/LES*, Columbus, OH. Greyden Press.
Speziale, C.G. (1998), "A combined large-eddy simulation and time-dependent RANS capability for high-speed compressible flows", *J. Sci. Comput.*, **13**(3), 253-274.
Steger, J.L. and Warming, R.F. (1981), "Flux vector splitting for the inviscid gas dynamic equations with applications to finite difference methods", *J. Comp. Phys.*, **40**(2), 263-293.
Travin, A., Shur, M., Strelets, M. and Spalart, P. (2000), "Detached-eddy simulation past a circular cylinder", *Flow Turbulence and Combustion*, **63**(1-4), 293-313.
van Leer, B. (1977), "Towards the ultimate conservative scheme. IV: A new approach to numerical convection", *J. Comp. Phys.*, **23**, 276-299.
Voke, P. (1997), "Flow past a square cylinder: test case LES 2", In Chollet J. *et al*. editors, *Direct and Large Eddy Simulation II*, vol. 5 of *ERCOFTAC Series,* pp. 355-373. Kluwer.

Appendix 1: Implicit time advancing

In the present section we show that when the simulation is advanced in time implicitly with the

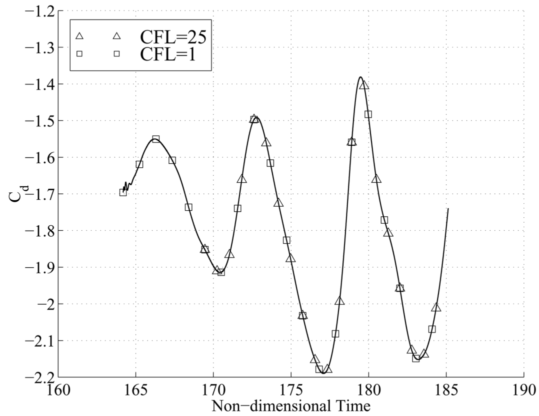

Fig. 7 Drag coefficient obtained with two simulations on grid GR3, using the LNS model, advanced in time explicitly (CFL=1) and implicitly (CFL=25) respectively

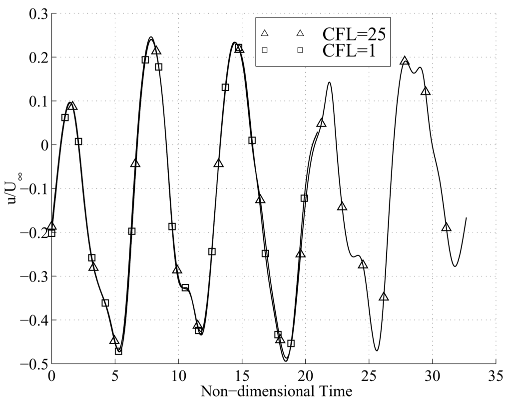

(a) u/U_∞

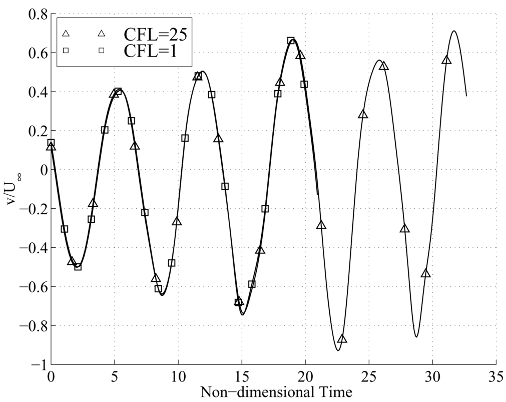

(b) v/U_∞

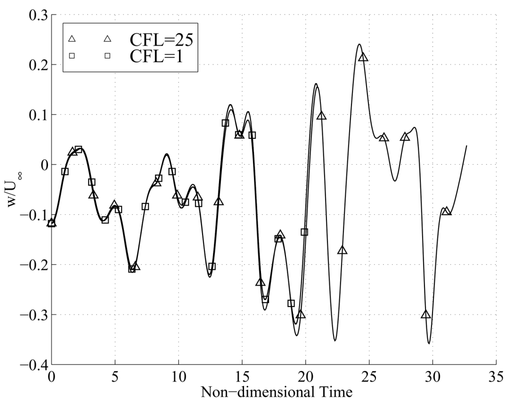

(c) w/U_∞

Fig. 8 Instantaneous velocity signals obtained in two simulations differing only for the time advancing (explicit with CFL=1 and implicit with CFL=25) at the point of coordinates *x*=1, *y*=0 and *z*=0 maximum CFL number equal to CFL=25, no significant information is lost with respect to the explicit time advancing (CFL=1). This has been checked by carrying out two LNS simulations on grid GR3, with the same numerical parameters and started from the same initial conditions, one advanced in time implicitly and the other explicitly. The behavior of the global forces obtained in implicit time advancing is the same as the one obtained in the explicit simulation, as can be seen for instance, in Fig. 7, in which the time variation of the drag coefficient is reported. Moreover, Fig. 8, which displays the instantaneous velocity components measured in a point located in the wake, shows that differences between implicit and explicit time advancing are negligible also on more local quantities.

The implicit algorithm is clearly more convenient than the explicit one. Indeed we have estimated that, for a given time interval, implicit simulations are 12 times faster than the explicit ones.

GS